Pure & Appl. Chem., Vol. 56, No. 9, pp. 1153-1165, 1984.
Printed in Great Britain.

0033-4545/84 $3.00+0.00
Pergamon Press Ltd.

THE PHOTOPHYSICS AND PHOTOCHEMISTRY OF THE PLANT PHOTOSENSOR PIGMENT PHYTOCHROME

Silvia E. Braslavsky

Max-Planck-Institut für Strahlenchemie, D-4330 Mülheim a. d. Ruhr, FRG.

Abstract - The similarity of the photophysical (*e. g.*, fluorescence lifetimes) and photochemical (*e. g.*, transients kinetic behaviour) properties determined for differently-sized phytochromes (small: 60 kD, large: *ca.* 114-118 kD, and native: 124 kD) indicates that the first steps of the photochromic transformation between the two thermally stable forms of the pigment, P(r) and P(fr), are reactions of the conjugated tetrapyrrole chromophore interacting with protein regions still present in small P(r). I(700), the primary photoproduct of P(r), with which it is in a photochromic equilibrium, decays biexponentially within microseconds. These and further dark steps of the transformation, taking place within milliseconds and even seconds, might be proton transfers, conformational changes of the chromophore and, in the last steps leading to P(fr), of the protein. A set of parallel reactions from P(r) to P(fr) can best fit the kinetic data available. In solution, the radiationless processes of the fully conjugated stretched tetrapyrroles (serving as chromophore models) mainly occur around the central C-10 methine group, while at an early stage during the P(r) → P(fr) photoconversion a *Z/E* isomerization takes place at the C-15 methine group of the chromophore. The protein therefore appears to impair the twisting around C-10, creating the very efficient energy wasting step responsible for the more than 80% heat loss after light absorption by P(r) and by P(fr).

INTRODUCTION

Photomorphogenesis is the control of plant development by light, independent of photosynthesis. There is a great number of photomorphogenetic responses in the plant world, like germination, etiolation, synthesis of chlorophyll, transport of sucrose, formation of hairs, production of enzymes, etc. (1). The common property of these responses is their photosensitivity, with maximum efficiencies at 665 ("red") and 730 ("far-red") nm. These wavelengths correspond to the absorption maxima of the two photochromic forms, P(r) and P(fr), respectively, of the photosensor protein phytochrome (Fig. 1) which

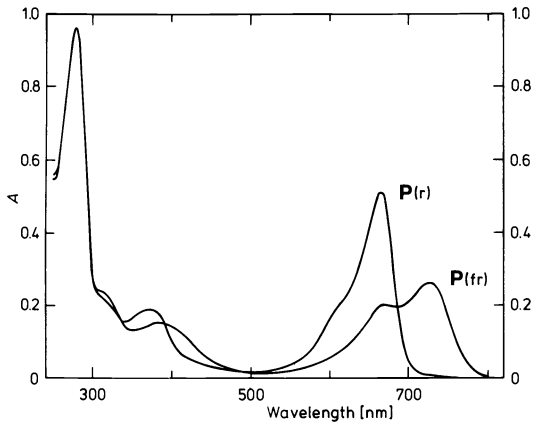

Fig. 1. Absorption spectra of highly purified 124 kD phytochrome in potassium phosphate buffer (pH 7.8) + 20% ethylene glycol (2).

enables plants to detect the light quality and intensity of the environment (*e. g.*, spectral properties, start and duration of the day) throughout their entire life cycle.

The comparison of the most recently isolated phytochrome of 124 kD (3-5) with the product of cell-free translation of phytochrome m-RNA indicates that the 124 kD form is indeed the native monomeric species (6). It is degradable to species of smaller molecular weight which have spectral properties slightly different from those of the action spectra (specially in the far-red form), but which retain photoreversibility. The degraded phytochrome preparations include a 60 kD photochromic piece (small phytochrome), isolated by conventional protein methods (7), and a mixture of 114 and 118 kD molecular masses (large phytochrome), isolated immunochemically (8).

While the constitution of P(r) is known to include a linear conjugated tetrapyrrole, a dihydrobilitriene (9-11) which is linked through a thioether bond

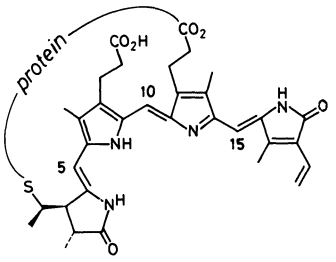

Fig. 2. Structure of phytochrome in its P(r) form (9-11).

to the protein (Fig. 2), the structure of the physiologically active form, P(fr) is not yet clearly established.

Only one tetrapyrrole chromophore is present per molecular unit of any of the different phytochrome forms (small, large, native) (11). Considering that bilitrienes in the absence of non-denatured protein do not exhibit a photochromism comparable to the P(r)-P(fr) interconversion, the nature of the protein-chromophore interactions and their influence on the photophysical and photochemical properties of the chromophore are of fundamental importance.

Calculations (12,13) as well as comparison with models of known geometry - porphyrins for a helically coiled form with a large ratio of the oscillator strengths, $D(UV)/D(Vis)$, and phorcabilin and isophorcabilin for a stretched form (small $D(UV)/D(Vis)$) (14) - led to the conclusion that the $D(UV)/D(Vis)$ ratio is an indication of the conformational extension of the conjugated tetrapyrrole backbone (15). Since this ratio is small in the case of both photochromic forms of the phytochromes, the chromophore is assumed to adopt a stretched conformation in either case.

In a chromopeptide fragment of eleven aminoacid residues, prepared by proteolytic digestion of P(r), the configuration around the three exocyclic methine bridges of the bilitriene was found to be *Z*. In the P(fr) chromopeptide prepared similarly, the double bond C-14,15 exhibits an *E* configuration. While the P(fr) fragment reverted to the P(r) chromopeptide on irradiation, the direct reverse photoconversion was not possible. It was concluded that during the photoconversion of the small, large, and native chromoprotein a $Z \rightarrow E$ isomerization at C-14,15 takes place (16,17) which in the chromopeptide fragment is possible only in one direction, P(fr) → P(r). However, the double bond isomerism alone cannot explain the spectral shifts between the two forms, since the P(fr) chromopeptide absorbs at a shorter wavelength than the P(r) one (in contrast to the native protein, see Fig. 1). Neither can the several intermediates produced during the transformation (18) be explained only on the basis of a one-step isomerization. These intermediates have been detected through their characteristic absorption spectra *in vitro* with small (19-21), large (22-26) and native (2) phytochromes as well as *in vivo* in etiolated tissues at low temperatures (27). The maxima lie between the maxima of the two stable forms and much has been speculated about their nature (16).

Several processes can lead to changes in the spectral properties of a bilitriene chromophore, *e. g.*, configurational and other conformational changes, proton transfer, electron transfer, and chemical modifications of the conjugated system such as addition-elimination reactions. Any of these could be significantly assisted by interactions with the surrounding protein. Each intermediate should be the result of one or a combination of more than one of these processes.

We have addressed ourselves to the question of the molecular basis of the P(r)

$\overleftrightarrow{P(fr)}$ photochromism through the study of

(a) the emission properties of the two forms,
(b) the radiationless processes and the calorimetry involved,
(c) the kinetics of the transformations, and
(d) the photophysics and photochemistry of the chromophore model compounds.

This paper constitutes a progress report. Native phytochrome has only recently been obtained in our laboratory (Fig. 1, (2)). Not all the measurements carried out previously with small and large phytochromes have been yet repeated with the more recent native protein (4).

THE EMISSION PROPERTIES OF PHYTOCHROME

The corrected fluorescence excitation spectra of small and large phytochrome are not totally in agreement with the absorption spectra (cf. Fig. 3).

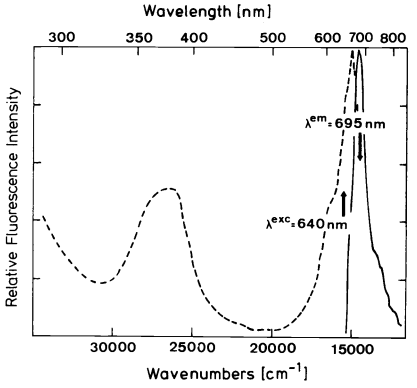

Fig. 3. Corrected fluorescence (——) and fluorescence excitation (---) spectra of large phytochrome in potassium phosphate buffer, pH 7.8, at 275 K (28).

As shown in Table 1, the fluorescence quantum yields ($\Phi(f)$) for large and small $P(r)$ are quite similar at 275 K (28). This result is at variance with a large difference reported earlier for 300 K (29,30). The difference in $\Phi(f)$ of both $P(r)$ preparations seems to depend somewhat on the excitation band.

TABLE 1. Fluorescence quantum yields of small (S) and large (L) phytochrome in potassium phosphate buffer (pH 7.8) at 275 K (28).

λ(exc)	$\Phi(f,exptl)\cdot 10^3$		$\Phi(f,corr)\cdot 10^{3a}$	
	S-P(r)	L-P(r)	S-P(r)	L-P(r)
640 nm	5 ± 1	3.3 ± 0.3	1.5 ± 0.3	2.0 ± 0.2
380 nm	3.4 ± 0.7	2.9 ± 0.3	-	-

[a] Corrected for impurity emission, see text.

This is consistent with the fact that the $D(UV)/D(Vis)$ ratio is larger in the excitation than in the absorption spectra. One possible reason may be the "anomalous" emission (Fig. 4) (31). It originates from a contaminant produced most probably upon addition of a nucleophile (from either the surrounding protein or the solvent) to C-10, the lowest-electron density position of the tetrapyrrole, affording a bilirubin-type chromophore with one of the dipyrrolic moieties exhibiting an absorption maximum at 380 nm and properties similar to those of a dipyrromethenone (half bilirubin). An analogous "anomalous" emission, due to a nucleophilic addition at C-10, has been found in the case of the model compound biliverdin dimethyl ester (32). It is not possible to correct for this contaminant since its absorbance is not known. Its contribution to the emission intensity in the blue region depends on the phytochrome type (Fig. 4). Since a dipyrromethenone, when associated to albumin, increases its emission yield about 25 times over that in solution (33), the emission efficiency of the "anomalous" emission is possibly also

large and the concentration of the contaminant low.

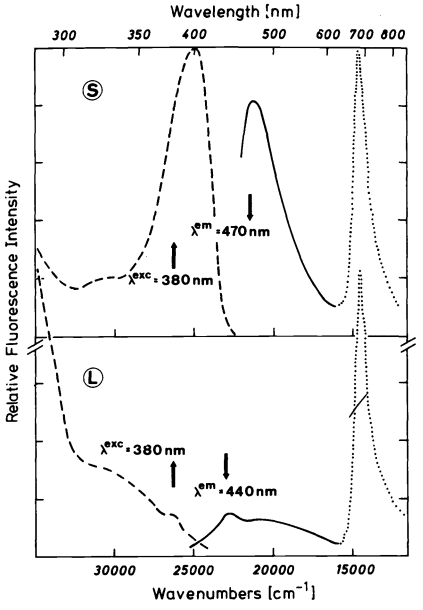

Fig. 4. Corrected spectra of the "anomalous" fluorescence of small and large phytochrome at 275 K in potassium phosphate buffer (pH 7.8). **S**: (——) "Anomalous" and (···) normal fluorescence, and (---) "anomalous" fluorescence excitation of small phytochrome. **L**: (——) "Anomalous" and (···) normal fluorescence, and (---) "anomalous" fluorescence excitation of large phytochrome (31).

Another possible reason for the difference between the absorption and the excitation spectra of P(r) is the presence of other red-emitting components different from intact phytochrome. These compounds were, in the large phytochrome samples, less than 10%, as revealed by component-resolved lifetime measurements. They have, however, longer lifetimes, thus contributing to up to 40% of the fluorescence intensity in the case of large P(r) and even more in the case of small P(r). The lifetime of the main component of the emission is 45 ps for both molecular weight samples at 275 K. With this value at hand and the relative contribution of this component to the total emission yield, the yield determined by static methods [Table 1: Φ(f,exptl)] could be corrected [Table 1: Φ(f,corr)]. The corrected value for large P(r) is in agreement with that reported by Hermann *et al.* for rye phytochrome at 293 K (34).

Considering that the radiative lifetime of P(r), calculated from the oscillator strength, is 20 ns (30) and that the experimentally determined lifetime is 45 ps, a theoretical quantum yield of 0.0023 can be deduced. This value is in line with the above-mentioned corrected yield obtained independently. In this manner, a consistent set of photophysical parameters could be calculated for small and large P(r). They do not differ at 275 K, which indicates that, at least at this temperature, the additional *ca.* 60 kD protein piece does not change the nature of the radiationless processes.

In a red-light equilibrated sample composed of P(r) and P(fr) the same main decay component was observed in the proportion expected for the 20% (35) of the P(r) component. A fluorescence lifetime of P(fr) could not be detected, most probably because it is considerably shorter than 20 ps. This indicates that the radiationless processes are faster in the physiologically active P(fr) form of the pigment than in the dormant P(r) form.

Taking into account that the overall photochemical yield of the P(r) → P(fr) conversion is between 0.1 and 0.2, depending on the molecular weight (4,36), and that the fluorescence yield is in the order of 0.001, more than 80% of the excitation energy is dissipated as heat. This can be studied through optoacoustic spectroscopy.

THE RADIATIONLESS PROCESSES OF P(r) and P(fr)

The action spectrum (optoacoustic spectrum, OAS) of the promptly dissipated heat at 275 K by a solution of small P(r) from oat upon excitation by 15 ns laser pulses of different wavelengths was determined by recording the acoustic wave generated in the medium (Fig. 5) (37,38).

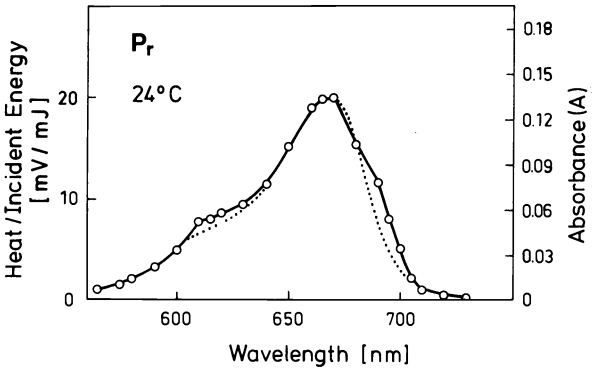

Fig. 5. Absorption spectrum (——) of small P(r) and action spectrum (···; normalized at 665 nm) of heat emission (OAS) after laser excitation (38).

Deviations of the OAS from the absorption spectrum around 610 and 700 nm indicate the build-up of photoproduct(s) absorbing part of the energy of the laser pulse and contributing to the heat evolved within the pulse duration and up to 0.5 μs, the time resolution of the experiment.

These experiments establish that

(a) I(700) (lumi-R), the transient characterized by flash photolysis of small (19-21), large (22-24), and native (2) P(r), representes the first intermediate stage in the path to P(fr) at 275 K,

(b) the photochromic relation between I(700) and P(r), which had already been demonstrated to exist in the large phytochrome system (39), is set up within 15 ns of the excitation of small P(r) (in fact, all experimental evidence indicates that the same mechanism of phototransformation operates in the differently-sized phytochromes; this important aspect will be discussed in more detail in the next section), and

(c) I(700) contains ca. 140 kJ/mol more internal energy than P(r) (Fig. 6).

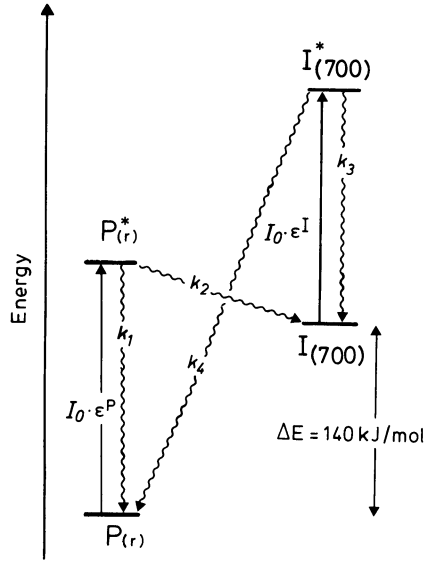

Fig. 6. State diagram of P(r) and the primary photoproduct I(700), including rate constants for physical and chemical excited-state deactivation, and the calculated internal energy content difference between P(r) and I(700). The values for lg k_1 and lg k_2 can be calculated as 10.3 and 9.5 (from k in 1/s), respectively (38).

This value was calculated assuming that the prompt heat dissipation around 590 nm (90% of the absorbed energy) is only due to P(r), with no contribution from the intermediates (note a), and that the quantum yield for the production of the first transient(s) is 0.13 for small P(r), *i. e.*, the same as that for the production of the final product, P(fr) (note b) (39). The heat measured after excitation at 590 nm thus includes the internal conversion of excited P(r) and the exothermicity involved in the production of the first intermediate(s).

The P(r) $\rightleftarrows$ I(700) photochromic system may play an important role in determining the final concentration of the species triggering the photomorphogenetic processes *in vivo*, at sufficiently high radiant power. This could be shown, *e. g.*, in germination induction experiments with lettuce seeds using laser pulses of different wavelengths (42): a 690 nm pulse initiated less germination than a 620 nm pulse, after due consideration of the differences in P(r) absorbance. This is explainable by the photoreversion of the first intermediate, I(700), within the 15 ns laser pulse to starting P(r), thus impairing the formation of P(fr). Similar conclusions were drawn from *in vivo* experiments using millisecond and microsecond flashes (43).

Since no "excess" heat is detected in any spectral region (Fig. 7), upon

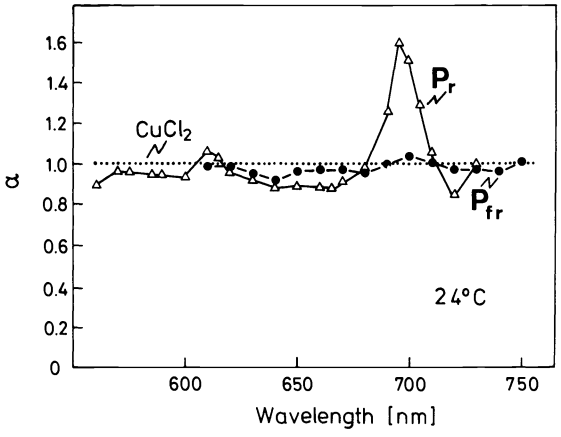

Fig. 7. Action spectra for heat emission (OAS) from laser-excited P(r) (-Δ-Δ-) and P(fr) (-●-●-), corrected for the absorbed light energy by calibration with copper chloride (···). The heat emission data for P(r) are taken from Fig. 5 (38).

irradiation of P(fr), either no early (< 0.5 μs) intermediates are formed or they do not lead to any prompt heat dissipation.

The difference between the heat emission and the absorption spectrum recorded for P(r) in the 610 nm region is due to either an absorption band of I(700) or another transient absorbing in this region. These two alternatives will be discussed in the next section.

Information about the primary photoprocesses of both final species can be obtained from a comparison of the prompt heat dissipations. On the one hand P(r) emits, upon excitation with 660 nm, about 10% less heat than P(fr) (Fig. 7). This may reflect the fact that the yield for P(r) → P(fr) is higher than that for the reverse reaction (35,36). On the other hand, the fact that the prompt heat dissipation by both final species is of the same order of magnitude and that P(fr) fluoresces at least ten times less efficiently than P(r) (28) means that the rate of internal conversion to ground state is larger for the former.

Note a: In the 590 nm wavelength region the transients essentially do not absorb, at least at low temperatures (26).
Note b: This value was calculated using the quantum yield for P(r) → P(fr) reported by Butler *et al.* (35), and the new value for ε(max, P(r)) recently obtained by Litts *et al.* (5) for native phytochrome. This absorption coefficient agrees with the values for small and large phytochromes (40,41).

Preliminary results on laser induced OAS of native P(r) indicate the same general features as those of small P(r). However, a quantitative comparison of the heat released is not yet possible (44).

THE KINETICS OF THE PHYTOCHROME PHOTOTRANSFORMATION

Although the occurrence of microsecond and millisecond intermediates in the phototransformation paths P(r) $\rightleftarrows$ P(fr) at different temperatures is well documented (16-27), there are open questions related to their structure, the activation parameters involved in the transformations, and the influence of the (variable) size of the protein attached to the chromophore.

Since the phototransformations are monophotonic all transients succeeding the first one must arise in dark reactions. It is generally accepted, although not definitively established, that the intersystem crossing yield in phytochrome is very small. The most rigorous arguments are derived from a comparison with the biliverdin model chromophore (45).

The time-resolved difference spectra obtained upon nanosecond laser excitation of small P(r) at 275 K are shown in Fig. 8.

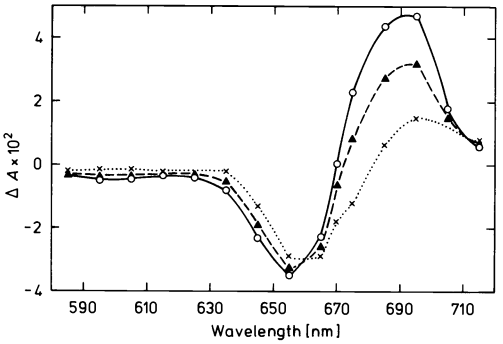

Fig. 8. Time resolved transient spectra taken immediately (—o—o—), 60 μs (-▲-▲-), and 1000 μs (·x·x·) after irradiation of small P(r) with 15 ns laser pulses. λ(exc) = 640 nm (2). The points were extracted from the decay traces. Each trace was an average of 25 decays.

The corresponding spectra obtained with large phytochrome are very similar (22,39), and the results from native phytochrome indicate that in this case the spectra are not different either (2).

The information on the kinetics of the phototransformation accumulated up to now favours parallel paths leading from P(r) to P(fr), at least *in vitro* at temperatures from 273 to 300 K. Scheme 1 explains the fast decays of the transients formed upon excitation of P(r). It includes the back phototransformation of I(700) (38,39,42,43). It is a modification of a scheme postulated to account also for the appearance of P(fr) (23).

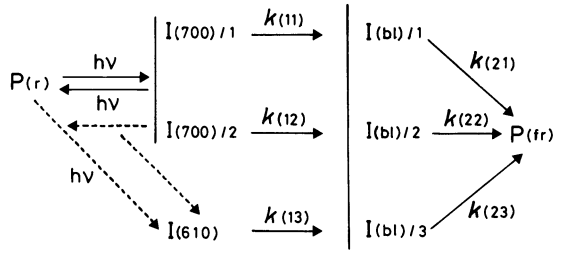

Scheme 1

I(700), also called lumi-R (18,27), represents the first absorbance difference immediately after the flash with an absorption maximum around 700 nm. According to the OAS studies (38), this species possesses 140 kJ/mol more internal energy content than the P(r) starting material.

From low temperature studies (46) it was concluded that the *Z* → *E* isomerization around C-14,15 takes place in the early stages of the P(r) → P(fr)

transformation. It could, in fact, be the primary photochemical step leading to I(700) within picoseconds. In scheme 1, the two species I(700)/1 and I(700)/2, rather than only one homogeneous I(700) primary product are made responsible for the biexponential decay, since there is no kinetic evidence in favour of a sequential scheme with I(700)/2 arising from I(700)/1.

In a kinetic analysis of the flash photolysis results of small and native P(r), the decay curves at different analyzing wavelengths were fitted for up to 2 ms with a sum-of-single-exponential-decays function, $F(t) = \sum A(i) \exp(-t/\tau(i))$ (47). The biexponential decay at 695 nm (maximum of the difference spectrum; see Fig. 8) was the same for the I(700) of both P(r)s, with lifetimes of 20 and 200 μs at 275 K and relative abundances of 0.4 and 0.6, respectively.

This indicates, in accordance with previous observations, that the first intermediates are modifications of the chromophore independent of the size of the whole protein. Judging from the similarity of the coefficients the existence of two decay paths from I(700) must be an inherent property of phytochrome and not, as suggested, a result of a heterogeneity in molecular size (23). Of course, one possibility is that in all phytochrome preparations (small, large, and native) two different isomers are contained. These isomers could be different orientations of the chromophore in the protein or two chromophore conformations. They would automatically lead to more than one set of intermediates even by the most simple linear mechanism. However, all available photophysical data suggest, albeit not conclusively, that there is an homogeneous phytochrome chromophore population. Alternatively then, the two decays could also derive from two different pathways of excited P(r) to two products, I(700)/1 and I(700)/2. Note that in this case $Z \rightarrow E$ isomerization could only be responsible for one of these intermediates, at best.

The activation parameters for the fast [$k(11)$] and slow [$k(12)$] decay components of I(700) for small and native P(r) in the temperature range 275-298 K are the same, $E(a) = 58 \pm 5$ kJ/mol and $\ln A = 35 \pm 1$ (A in 1/s units). This further supports that the degradation of native to small P(r) does not affect the chromophore site in the protein (2).

Most probably the further steps in the P(r) → P(fr) transformation involve proton transfer(s) and/or conformational changes of the chromophore and, in the last stages leading to P(fr), of the protein. Circular dichroism measurements within the protein absorption band have not shown a difference indicative of a change in conformation of the aromatic aminoacids upon phototransformation (12). The protein changes might be too small to be detected by this method.

I(bl) (Scheme 1) is a bleached intermediate with a lower absorption coefficient in the red spectral region, which was suggested to decay with three rate constants to P(fr) to account for the stepwise appearance of the latter (23). It has also been called meta-Rb (18), and its low red absorption coefficient (26) has been interpreted in terms of a helically coiled chromophore conformation similar to that adopted by free bilitrienes. It was further speculated that, in the process of this transformation, the chromophore partially detaches itself from the protein (perhaps loosing a hydrogen bridge) to reaccommodate into the P(fr) situation (12). At low temperatures and under dehydrating conditions another intermediate (meta-Ra) seems to be produced between lumi-R and I(bl) (16,18).

It is not known whether the protein size has any influence on the later steps of the transformation leading to P(fr). The question remains to be studied.

No bleaching mirror image of the P(r) absorption is observed in the 610-620 nm region in the difference spectra recorded directly after flash irradiation (2,19-23,39). This can be attributed to either of two reasons:

(i) The disappearance of P(r) absorbance is compensated by a concomitant increase in transient absorbance. This would be consistent with the difference between the optoacoustic and the absorption spectra in this region (Fig. 5). However, the absorbance differences at 695 nm and around 620 nm exhibit different kinetic behaviours. The decrease in the 695 nm region is coupled to (*i. e.*, occurring with the same kinetics as) a very small increase around 620 nm for small and native P(r) (2). This could only be discovered through the use of our signal averaging facilities and data analysis programs, considering the very small absorbance changes observed (ΔA *ca.* 0.001). The differences in both regions, therefore, may well be attributed to two different sets of

species, both primary photoproducts of P(r), *i. e.*, the I(700)s and another one, (I(610)), with an absorption maximum at 610 nm and a lifetime in the millisecond range. Within the frame of this interpretation, either I(700) would, in turn, have to convert also into I(610) at a later stage in order to explain the delayed increase in this region, or there is a partial back reversion in the dark of both I(700)s to P(r).

(ii) The disappearance of P(r) absorbance is compensated for by an increase in I(700) absorbance, the decay of which cannot be observed because I(700), in turn, proceeds to a transient having similar absorption coefficients as I(700) in this spectral region (26). The above-mentioned increase at around 610 nm would mean, in the frame of this interpretation, that I(b1), the transient produced from I(700), has a slightly larger absorption coefficient in this region.

Both interpretations need accidental correspondence, within the detection limits, of the absorbance at around 610-620 nm of two (case i) and even three (case ii) molecular entities. The first interpretation, however, would be more in accordance with the observation of the stepwise appearance of P(fr) (23). Such a behaviour can only be accommodated by a parallel set of reactions transforming P(r) to P(fr) (Scheme 1) including an I(610) intermediate.

THE PHOTOPHYSICS AND PHOTOCHEMISTRY OF THE CHROMOPHORE MODEL COMPOUNDS

The molecular characterization of the intermediates will only be possible through a detailed understanding of the photophysical and photochemical properties of model compounds. Pursuing this purpose, we chose biliverdin dimethyl ester (BVE) which differs from the phytochrome chromophore in the degree of saturation of one of the terminal rings (Fig. 9).

Our work of the past years on this subject, recently reviewed (48), shall be outlined briefly here.

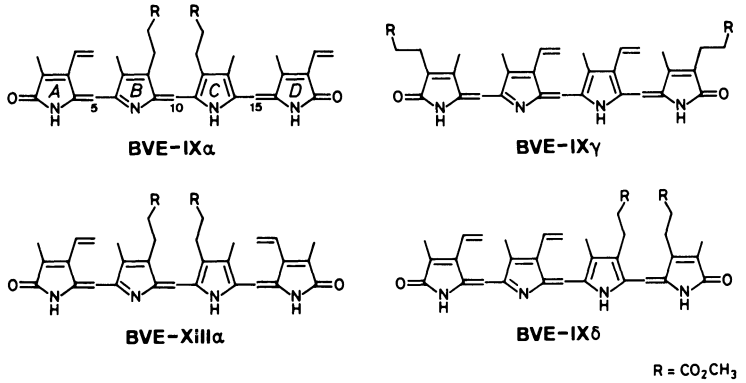

Fig. 9. Constitution of the dimethyl esters of biliverdin IXα (BVE), XIIIα, IXγ, and IXδ.

Using ^{1}H-NMR, absorption, fluorescence, fluorescence excitation, and medium induced circular dichroism of BVE, its protonated form, and of some of its constitutional isomers (*e. g.*, of BVE-XIIIα), it was shown that in diluted solutions, and when embedded in lipid membranes, bilitrienes are present in two forms. In neutral solutions one of the forms, helically coiled *Z*-syn,-*Z*-syn,*Z*-syn, emits in the far-red (around 710 nm), shows a large induced circular dichroism, a large *D*(UV)/*D*(Vis) ratio in the fluorescence excitation spectrum, and a large Stokes shift. The other one, a stretched (family of) form(s) emits in the red (around 660 nm), shows a poor induced circular dichroism, a smaller *D*(UV)/*D*(Vis) ratio in the fluorescence excitation spectrum as well as a narrower and more structured red excitation band, and a smaller Stokes shift. The relative population of the various forms is medium and temperature dependent (49,50).

Picosecond spectroscopy has helped to understand the nature of the radiationless processes undergone by the two forms of BVE (51). The helically coiled short-lived (ps lifetimes) lose their energy through proton transfer (intramolecular oscillation between the nitrogens of rings B and C) and conformational changes, such as twisting around the bonds linking the rings, most probably around the C-10 methine groups.

The stretched forms are more rigid, their lifetime being in the nanosecond time range. This rigidity is an inherent property of the bilitriene skeleton (*i. e*, the protein is not needed for this purpose). The relaxation processes of the stretched skeletons are *E,Z* isomerizations occurring selectively at the C-10 position, as was concluded in a study of the photocyclization of the BVE-IXγ and -IXδ isomers (Fig. 9), possessing a vinyl group adjacent to C-10 (48,52,53). These are the only isomers undergoing this type of photocyclization, yielding phorcabilin and neobiliverdin IXδ (NVE-IXδ), respectively (see Figs. 10,11). The reaction exhibits a strong ground state conformation-selective reactivity, as evidenced by a marked wavelength dependency. The reaction efficiency is the highest at the wavelengths where the stretched conformers absorb (*ca.* 580 nm) and decreases drastically at 640 nm, which is the maximum of the absorption envelope, and at which wavelength the stretched species do not appreciably absorb (Fig. 10).

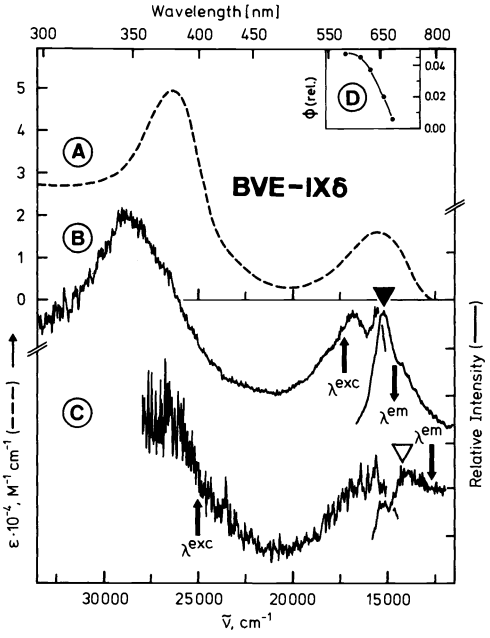

Fig. 10. Corrected fluorescence and fluorescence excitation spectra of BVE-IXδ in dimethylsulfoxide (0.000033 M) at room temperature. B: Predominantly stretched BVE-IXδ; C: predominantly coiled BVE-IXδ. A: Absorption spectrum. The amplitude of the longer-wavelength emission band (C: ▽) is *ca.* 0.05 of that of the shorter-wavelength band (B: ▼). D: Relative quantum yield, $\Phi(rel)$, for the formation of NVE-IXδ, as a function of irradiation wavelength (53).

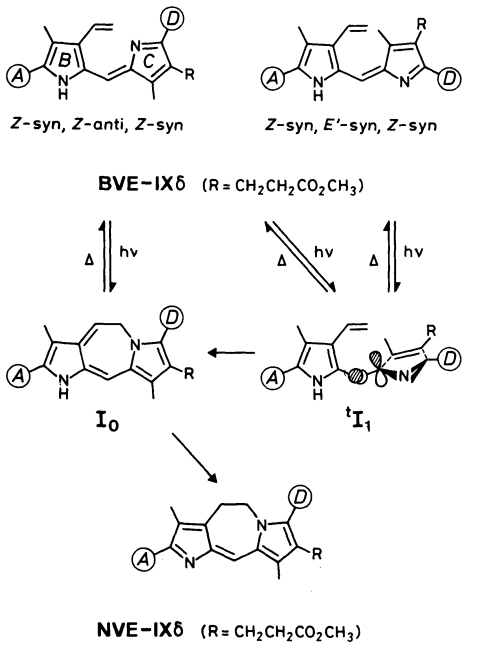

Fig. 11. Possible primary steps of the photocyclization of stretched forms of BVE-IXδ to neobiliverdin IXδ (NVE-IXδ). No change in symmetry takes place within the partial structures *A/B* and *C/D* (48,53).

This is undoubtedly due to the substantial predominance of the far-red absorbing coiled conformation above 630 nm and, implicitly, to the greater reaction efficiency of the stretched species. The absorption spectrum of each species

is revealed by the fluorescence excitation spectrum (Fig. 10B and C). Since the coiled species is the most abundant in most solvents, the absorption spectrum (Fig. 10A) is essentially that of this form.

In dimethylsulfoxide the efficiency of photocyclization is the highest. This is a consequence not only of the higher relative abundance of stretched species in this medium, but possibly also of a better stabilization of the excited state and of the ability of dimethylsulfoxide to facilitate the proton transfer needed to arrive to the final product (Fig. 11) (53). The quantum yield calculated on the basis of the absorption envelope is very low (ca. 0.00001) (52). However, this value does not consider the (unknown) relative population of the reactive species. Thus, an evaluation of the absolute efficiency of the photocyclization is not possible at the moment.

In the case of BVE-IXα, photolysis at low temperatures leads to changes in the absorption spectrum which disappear on heating to room temperature (49). While on irradiating at room temperature no spectral changes are observed, laser induced OAS has shown that at high dilutions a short-lived energy storing species is formed, which returns to the ground starting material with lifetimes shorter than milliseconds (54). This species should be the C-10 *E* isomer.

CONCLUSIONS AND FURTHER CONSIDERATIONS

The results of the photochemistry of the biliverdins can be rationalized by assuming that in each case the stretching of the coiled form is confined to transformations within the *B/C* moiety while the geometry around the other two bridges is retained. In the case of the stretched bilitriene skeleton the 10*Z* → 10*E* isomerization plays an appreciable role as a radiationless deactivation process.

The fluorescence lifetime of the stretched BVE form is ca. 1.9 ns (51), similar to that of C-phycocyanin (55). Although in both cases the chromophore is in a stretched conformation, the similarity in lifetimes should not any more be speculated upon for the moment, since the high flexibility of the bilitriene skeleton can lead to several possible stretched forms exhibiting similar lifetimes. The value of 10.3 for lg k_1 [Fig. 6; the internal conversion rate constant of excited P(r)], calculated from the fluorescence lifetime of 45 ps (28) and the prompt heat dissipation (38), indicates that a chromophore-protein interaction leading to an efficient energy wasting step occurs in the case of phytochrome (small and large). This process does not seem to play an important role in the case of C-phycocyanin.

While no photochemical reaction at C-5 or C-15 of the bilitrienes could be found, such reactions occur in the bilirubin chromophore which is saturated at C-10 (48,56), in bilirubin-type chromophores produced by nucleophilic addition to C-10 of verdins (57), and in C-10 rigid molecules, *e. g.*, phorcabilin (58,59). The *E* isomers obtained in the first two cases are more stable and much longer-lived than the C-10 geometrical isomers of the verdins, detectable only either at low temperatures or, indirectly (49,54), at room temperature.

The fact that at some stage during the P(r) → P(fr) transformation [between P(r) and I(bl) (47)] a C-15 isomerization should take place (16) must be related to the already mentioned protein-chromophore interactions, which inhibit the movement within the B/C moiety. Hydrogen bridges between the nitrogens of rings *B* and *C* and aminoacid groups might keep the *B/C* moiety of the phytochrome chromophore in an rigid conformation, thus impairing twisting around C-10 and creating, as a sacrificing process, the very efficient energy wasting step (hydrogen oscillations) responsible for the more than 80% heat loss after the absorption of light. This mechanism might have evolved out of the necessity to provide for longer-lived species, able to interact with the protein or, eventually, with other cellular parts (60). The increase of P(r) fluorescence yield in deuterated medium would be consistent with this interpretation (61).

Finally, the chromophore-protein interactions must take place in regions still preserved in small phytochrome, since the photophysics and the transient kinetics in the earlier stages of the P(r) → P(fr) transformation - when the chromophore transformations take place (16) - are independent of the protein size.

Acknowledgments The results and conclusions presented are the product of the collaborative effort of many scientists and technical assistants in Professor K. Schaffner's laboratory, who have developed the ideas exposed and

the methods used in the course of the past years. Many of them are listed as coauthors of the papers cited. Dr. A. R. Holzwarth and his coworkers are the main contributors in the emission work. Without this joint and interdisciplinary effort this work would have been impossible. We are specially indebted to the Computer Department of our Institute and to Mr. K. Mitterer for the development of the data acquisition and evaluation programs used in the flash photolysis and optoacoustic experiments, and to Professor E. Schäfer, Freiburg, and his group for the provision of small and large phytochromes.

REFERENCES

1. a) H. Smith, *Phytochrome and Photomorphogenesis*, McGraw-Hill, London (1975).
   b) H. Mohr, *Endeavour* New Series, *1*, 107-114 (1977).
2. B. Ruzsicska, S. Culshaw, S. E. Braslavsky and K. Schaffner, in preparation.
3. R. D. Vierstra and P. H. Quail, *Biochem. 22*, 2498-2505 (1983).
4. R. D. Vierstra and P. H. Quail, *Plant Physiol. 72*, 264-267 (1983).
5. J. C. Litts, J. M. Kelly and J. C. Lagarias, *J. Biol. Chem. 258*, 11025-11031 (1983).
6. G. W. Bolton, P. H. Quail, *Planta 155*, 212-217 (1982).
7. W. O. Smith, Jr. In *Photomorphogenesis*; W. Shropshire, Jr. and H. Mohr, eds.; *Encyclopedia of Plant Physiology, New Series 16A*. p. 96-118, Springer Verlag, (1983).
8. R. E. Hunt and L. H. Pratt, *Plant Physiol. 64*, 332-336 (1979).
9. J. C. Lagarias and H. Rapoport, *J. Am. Chem. Soc. 102*, 4821-4828 (1980).
10. L. H. Pratt, *Photochem. Photobiol. 27*, 81-105 (1978).
11. W. Rüdiger, *Structure and Bonding 40*, 101-140 (1980).
12. M. J. Burke, D. C. Pratt and A. Moscowitz, *Biochem. 11*, 4025-4031 (1972).
13. a) G. Wagnière and G. Blauer, *J. Am. Chem. Soc. 98*, 7806-7810 (1976).
   b) Q. Chae and P.-S. Song, *J. Am. Chem. Soc. 97*, 4176-4179 (1975).
   c) T. Sugimoto, K. Ishikawa and H. Suzuki, *J. Phys. Soc. Jpn. 40* 258-266 (1976).
   d) H. Falk and N. Müller, *Tetrahedron 39*, 1875-1885 (1983).
14. C. Pétrier, C. Dupuy, P. Jardon and R. Gautron, *Nouv. J. Chim. 6*, 495-503 (1982).
15. H. Scheer, *Angew. Chem. 93*, 230-250 (1981); *Angew. Chem. Intern. Ed. Engl. 20*, 241-261 (1981).
16. W. Rüdiger, *Phil. Trans. R. Soc. London B 303*, 377-386 (1983).
17. F. Thümmler and W. Rüdiger, *Tetrahedron 39*, 1943-1951 (1983).
18. R. E. Kendrick and J. de Kok, *Sci. Prog. Oxf. 68*, 475-486 (1983).
19. S. E. Braslavsky, J. I. Matthews, H.-J. Herbert, J. de Kok, C. J. P. Spruit and K. Schaffner, *Photochem. Photobiol. 31*, 417-420 (1980).
20. D. R. Cross, H. Linschitz and V. Kasche, J. Tenenbaum, *Proc. Natl. Acad Sci. 61*, 1095-1101 (1968).
21. L. H. Pratt and W. L. Butler, *Photochem. Photobiol. 11*, 361-369 (1970).
22. M.-M. Cordonnier, P. Mathis and L. H. Pratt, *Photochem. Photobiol. 34*, 733-740 (1981).
23. L. H. Pratt, Y. Shimazaki, Y. Inoue and M. Furuya, *Photochem. Photobiol. 36*, 471-477 (1982).
24. Y. Shimazaki, Y. Inoue, K. T. Yamamoto and M. Furuya, *Plant Cell Physiol. 21*, 1619-1625 (1980).
25. P.-S. Song, H. K. Sarkar, I.-S. Kim and K. L. Poff, *Biochim. Biophys. Acta 635*, 369-382 (1981).
26. W. Rüdiger and F. Thümmler, *Physiol. Plant. 60*, in press (1984).
27. R. E. Kendrick and C. J. P. Spruit, *Photochem. Photobiol. 26*, 201-214 (1977).
28. J. Wendler, A. R. Holzwarth, S. E. Braslavsky and K. Schaffner, *Biochim. Biophys. Acta*, in press (1984).
29. P.-S. Song, Q. Chae and W. R. Briggs, *Photochem. Photobiol. 22*, 75-76 (1975).
30. P.-S. Song, Q. Chae and J. D. Gardner, *Biochim. Biophys. Acta 576* 479-495 (1979).
31. A. R. Holzwarth, S. E. Braslavsky, S. Culshaw and K. Schaffner, *Photochem. Photobiol. 36*, 581-584 (1982).
32. S. E. Braslavsky, A. R. Holzwarth, H. Lehner and K. Schaffner, *Helv. Chim. Acta 61*, 2219-2222 (1978).
33. A. A. Lamola, S. E. Braslavsky, K. Schaffner and D. A. Lightner *Photochem. Photobiol. 37*, 263-270 (1983).
34. G. Hermann, B. Kirchhof, K. J. Appenroth and E. Müller, *Biochem. Physiol. Pflanz. 178*, 177-181 (1983).
35. W. L. Butler, S. B. Hendricks and H. W. Siegelman, *Photochem.*

Photobiol. 3, 521-528 (1964).
36. L. H. Pratt, *Photochem Photobiol. 22*, 33-36 (1975).
37. M. Jabben, S. E. Braslavsky and K. Schaffner, *J. Phys. 44 C-6*, 389-396 (1983).
38. M. Jabben, K. Heihoff, S. E. Braslavsky and K. Schaffner, *Photochem. Photobiol.*, in press (1984).
39. L. H. Pratt, Y. Inoue and M. Furuya, *Photochem. Photobiol. 39*, 241-246 (1984).
40. T. Brandlmeier, H. Scheer and W. Rüdiger, *Z. Naturforsch. 36 C*, 431-439 (1981).
41. S. J. Roux, K. McEntire and W. E. Brown, *Photochem. Photobiol. 35*, 537-543 (1982).
42. R. Scheuerlein and S. E. Braslavsky, in preparation (1984).
43. M. Kraml and E. Schäfer, *Photochem. Photobiol. 38*, 461-467 (1983).
44. K. Heihoff, unpublished results.
45. E. J. Land, *Photochem. Photobiol. 29*, 483-487 (1979).
46. F. Thümmler and W. Rüdiger, *Physiol. Plantarum 60*, in press (1984).
47. The fitting program was adapted from that developed by J. Wendler and A. R. Holzwarth for the evaluation of fluorescence decays. In preparation (1984).
48. S. E. Braslavsky, A. R. Holzwarth and K. Schaffner, *Angew. Chem. 95*, 670-689 (1983); *Angew. Chem. Int Ed. 22*, 656-674 (1983).
49. S. E. Braslavsky, A. R. Holzwarth, E. Langer, H. Lehner, J. I. Matthews and K. Schaffner, *Isr. J. Chem. 20*, 196-202 (1980).
50. I.-M. Tegmo-Larsson, S. E. Braslavsky, S. Culshaw, R. M. Ellul, C. Nicolau and K. Schaffner, *J. Am. Chem. Soc. 103*, 7152-7158 (1981).
51. A. R. Holzwarth, J. Wendler, K. Schaffner, V. Sundström, A. Sandström, and T. Gillbro, *Isr. J. Chem. 23*, 223-231 (1983).
52. M. Bois-Choussy and M. Barbier, *Helv. Chim. Acta 63*, 1098-1109 (1980).
53. S. E. Braslavsky, H. Al-Ekabi, C. Pétrier and K. Schaffner, *J. Am. Chem. Soc.*, in preparation (1984).
54. S. E. Braslavsky, R. M. Ellul, R. G. Weiss, H. Al-Ekabi and K. Schaffner, *Tetrahedron 39*, 1909-1913 (1983).
55. A. R. Holzwarth, J. Wendler and W. Wehrmeyer, *Photochem. Photobiol. 36*, 479-487 (1982).
56. A. F. McDonagh, L. A. Palma, F. R. Trull and D. A. Lightner, *J. Am. Chem. Soc. 104*, 6865-6867 (1982), and references therein.
57. H. Falk, N. Müller and T. Schlederer, *Monatsh. Chemie 111*, 159-175 (1980).
58. M. Choussy and M. Barbier, *C. R. Acad. Sc. Paris C-282*, 619-622 (1976).
59. M. Barbier, *Experientia 37*, 1060-1062 (1981).
60. W. Rüdiger and S. E. Braslavsky, unpublished.
61. H. K. Sarkar and P.-S. Song, *Biochem. 20*, 4315-4320 (1981).